Supplemental Materials

Molecular Biology of the Cell

Yue *et al*.

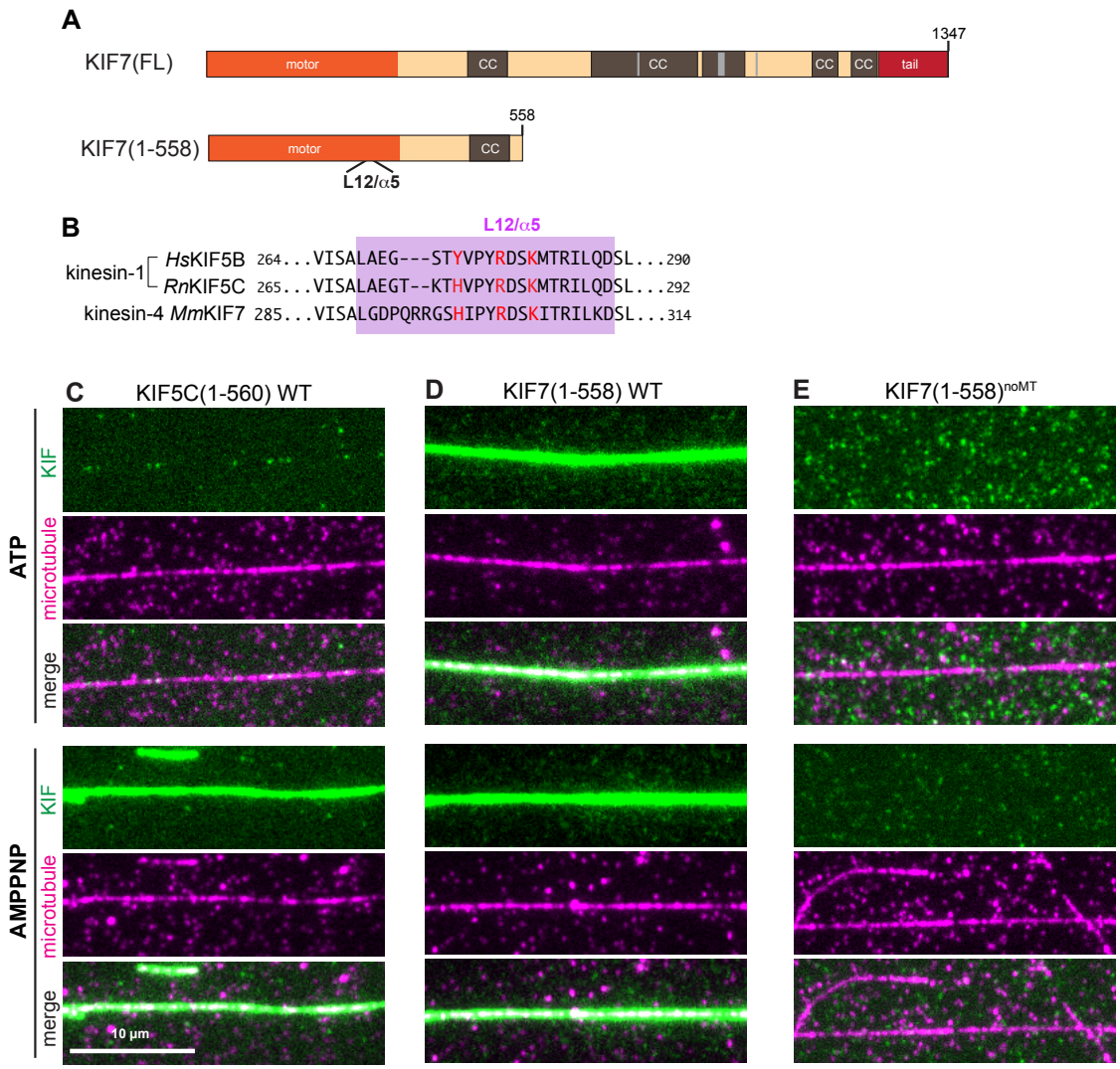

Figure S1: The KIF7(1-558)^{noMT} mutant lacks microtubule binding ability.

(A) Schematic of the domain organization of KIF7(FL) and truncated (1-558) proteins. Full-length KIF7 does not bind to microtubules because it is in an autoinhibited state (Blasius et al., 2021) and thus, to test whether specific mutations can abolish KIF7's ability to bind to microtubules, we utilized the truncated version (amino acids 1-558) that retains the kinesin motor domain and the first coiled-coil segment for dimerization and is active for microtubule binding in cells and in single-molecule in vitro assays (He et al., 2014; Yue et al., 2018).

(B) Sequence alignment of the L12/α5 region of KIF7 with that of the kinesin-1 motors KIF5B and KIF5C. Purple shaded region indicates the L12/α5 region. The red letters indicate the residues in KIF5B that abolish microtubule binding when mutated to Alanine (Woehlke *et al*., 1997) and equivalent positions in KIF5C and KIF7.

(C-E) Fluorescence-based microtubule binding assay. Representative images of mNeonGreen (mNG)-tagged (D) KIF7(1-558) WT and (E)KIF7(1-558)^{noMT} motors (green) bound to taxol-stabilized HiLyte647-labeled microtubules (magenta) in the presence of ATP (top) or the non-hydrolyzable ATP analogue AMPPNP (bottom). KIF7(1-558) displayed high affinity for microtubules in the presence of ATP and AMPPNP, consistent with previous work (He *et al.*, 2014; Jiang *et al.*, 2019; Yue *et al.*, 2018). In contrast, the KIF7(1-558)^{noMT} mutant protein did not bind to microtubules in either nucleotide state. (C) The kinesin-1 KIF5C(1-560)-mNG was used as a control as it displays a >20-fold higher affinity for microtubules in the presence of AMPPNP than in the presence of ATP (Crevel *et al*, 1996). Scale bar, 10 µm.

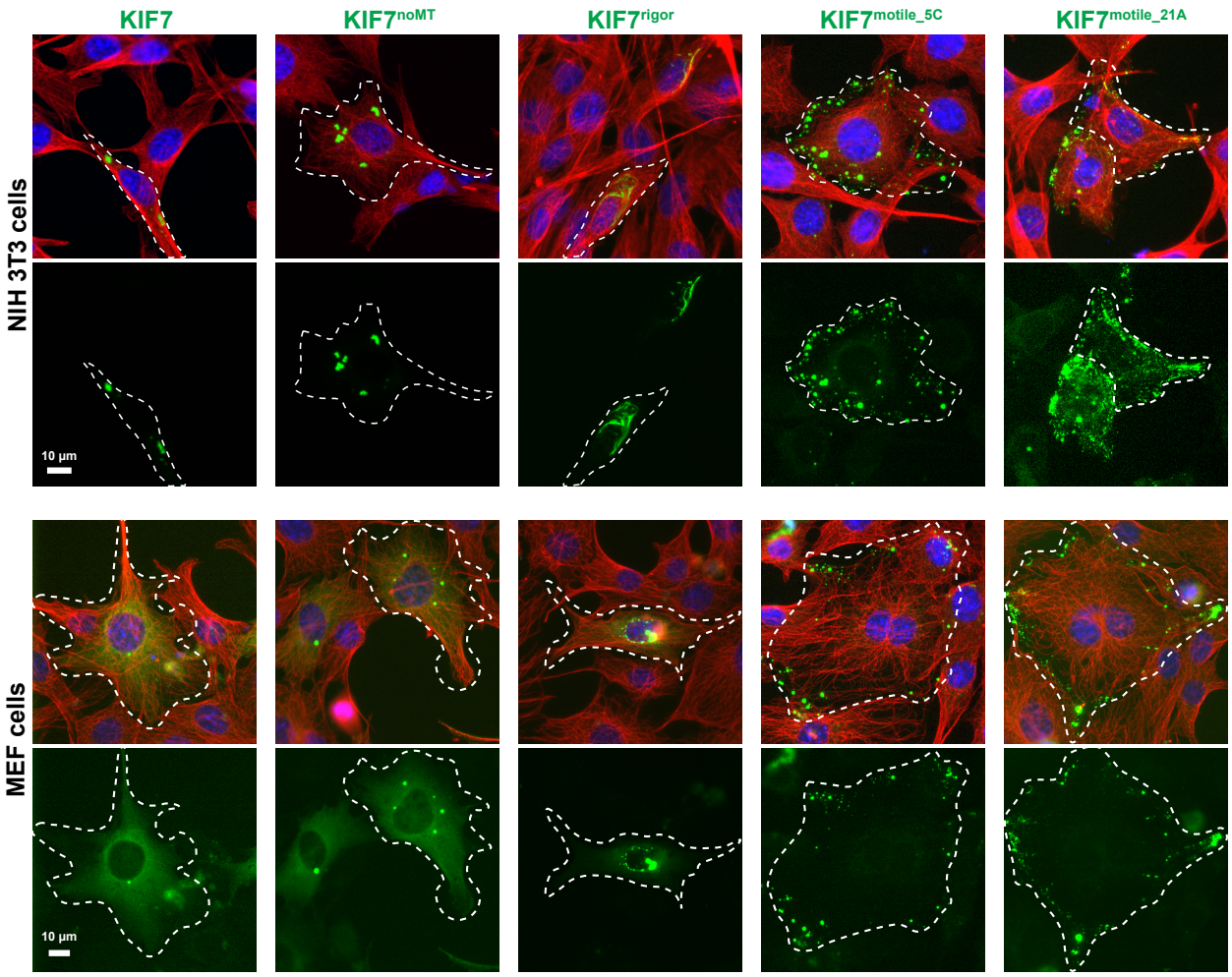

Figure S2: Localization of KIF7-mCit WT and variants expressed in (A) NIH 3T3 and (B) MEF cells. All KIF7 proteins were tagged at their C-termini with mCit (green). The cells were fixed and stained with antibodies against β-tubulin to mark microtubules (red) and with DAPI to mark the nucleus (blue). White dashed lines indicate the periphery of representative transfected cells. Scale bars, 10 µm.

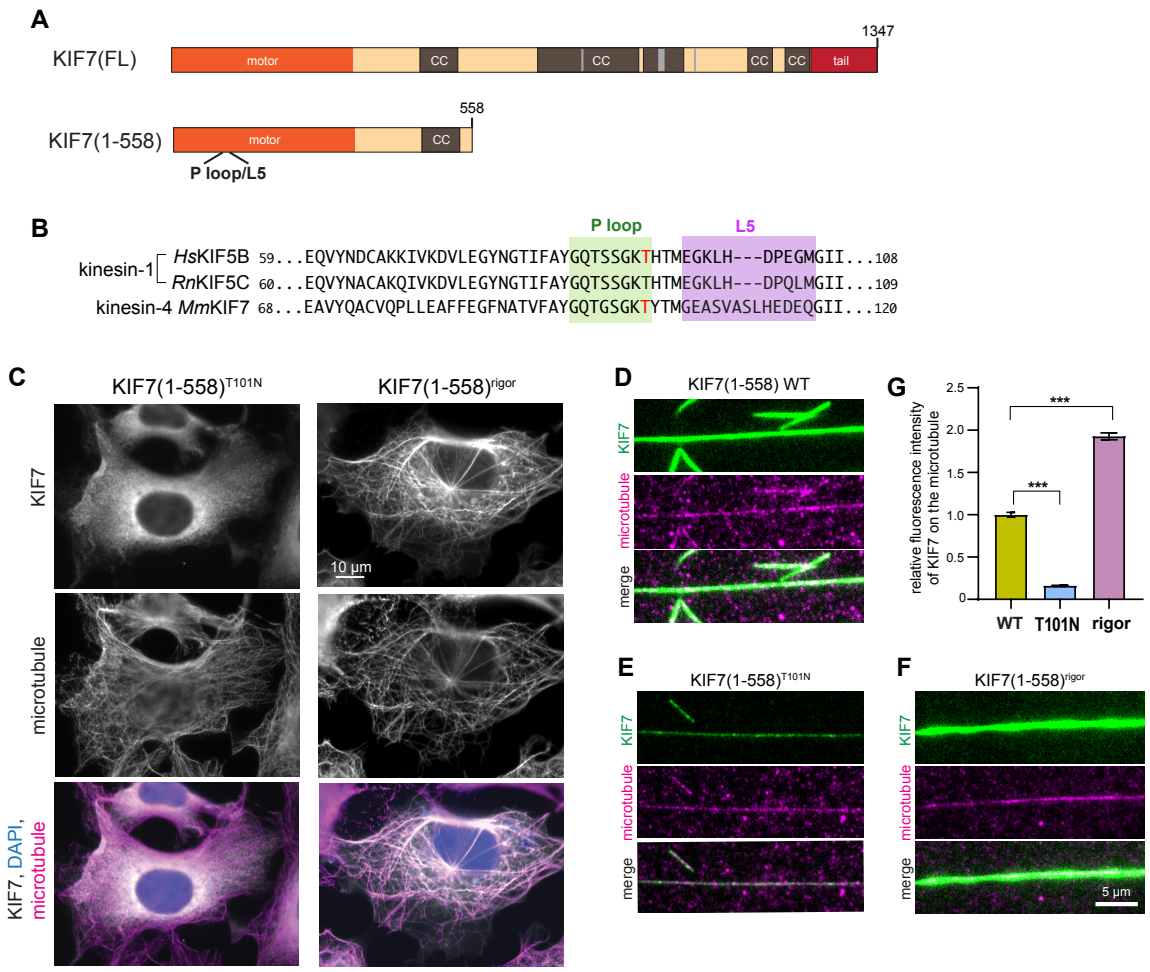

Figure S3: The KIF7(1-558)^{rigor} variant binds strongly to microtubules.

(A) Schematic of the domain structure of FL and truncated (1-558) KIF7. Full-length KIF7 does not bind to microtubules because it is in an autoinhibited state (Blasius et al., 2021) and thus, to test whether specific mutations can abolish KIF7's ability to bind to microtubules, we utilized the truncated version (1-558) that retains the kinesin motor domain and the first coiled-coil segment for dimerization and is active for microtubule binding in cells and in single-molecule in vitro assays (He et al., 2014; Yue et al., 2018).

(B) Sequence alignment of the P loop and L5 regions of KIF7 with that of the kinesin-1 motors KIF5B and KIF5C. Green-shaded region indicates the P loop with the red text indicating Threonine to Asparagine mutation in the KIF5B rigor mutant (Nakata *et al*., 1995) and the equivalent mutation in the KIF7^{T101N} mutant. The purple-shaded region indicates L5 and the residues of KIF7 that were replaced by those of KIF5C in the rigor mutant.

(C) KIF7(1-558)^{rigor} but not KIF7(1-558)^{T101N} can bind to microtubules in cells. Representative images of mCit-tagged KIF7(1-558)^{T101N} and KIF7(1-558)^{rigor} mutants expressed in COS-7 cells. The cells were fixed and stained with antibodies against β-tubulin to mark microtubules (magenta) and with DAPI to mark the nucleus (blue). Scale bar, 10 µm.

(D-G) Fluorescence-based microtubule binding assay. Representative images of mCit-tagged (D) KIF7(1-558) WT, (E) KIF7(1-558)^{T101N}, or (F) KIF7(1-558)^{rigor} motors (green) bound to taxol-stabilized HiLyte647-labeled microtubules (magenta) in the presence of ATP. Scale bar, 5 µm. (G) Quantification of the mean fluorescence intensity of the mutant motors normalized to that of the WT motor. The KIF7(1-558)^{T101N} mutation caused a >6-fold decrease whereas the KIF7(1-558)^{rigor} mutation caused an ~2-fold increase in the affinity of KIF7(1-558) for microtubules. ***, P<0.001 as compared to WT (two-tailed *t* test). Data are described as mean ± SEM of >78 microtubules from two independent experiments.

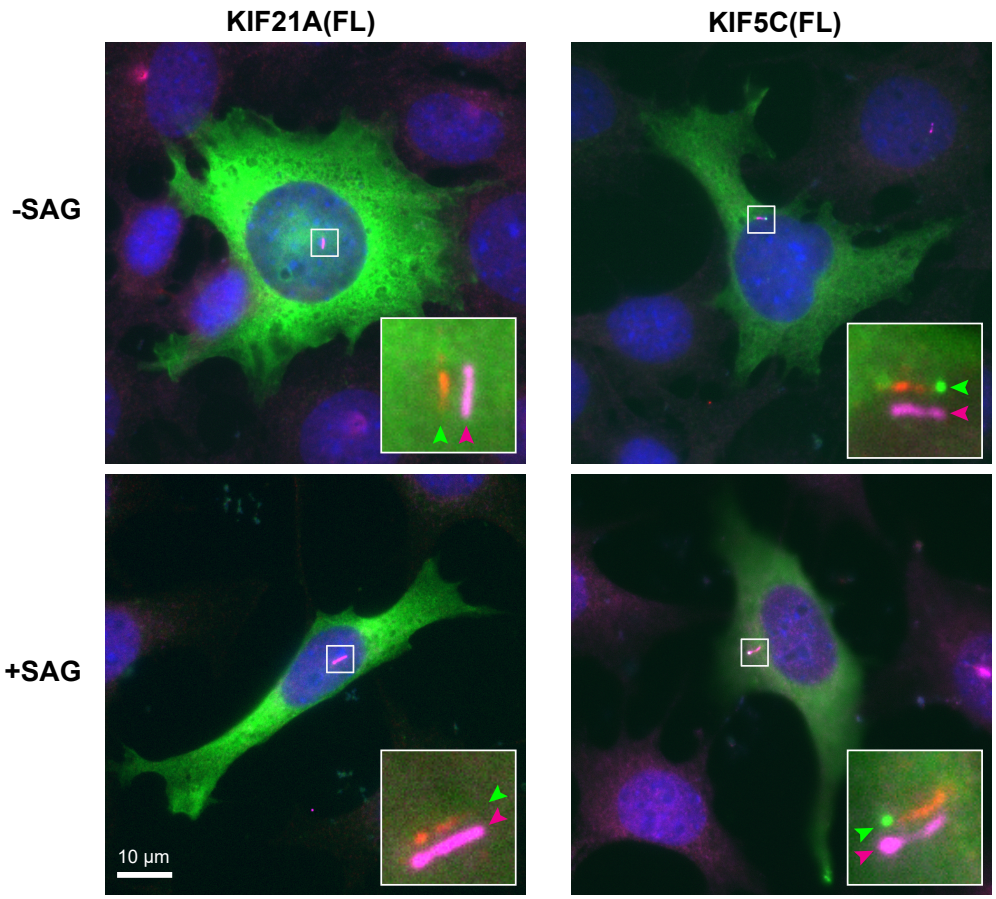

Figure S4. Ciliary localization of the kinesin-1 KIF5C and kinesin-4 KIF21A motors. *Kif7*$^{-/-}$ MEFs were transfected with plasmids for expression of GFP-KIF21A (left panels) or KIF5C-mCit (right panels). The cells were untreated (-SAG) or were treated with 400 nM SAG for 4 h (+SAG) to stimulate the Hh pathway. The cells were fixed and stained with DAPI to mark the nuclei (blue) and with antibodies against Arl13b to mark the primary cilium (magenta) and polyglutamylated tubulin to mark the cilium base (red). Inserts show magnification of the area outlined by the white box with the fluorescence signals offset by 15 pixels for clarity. Arrowheads indicate the tips of cilia. Scale bar, 10 µm.